Displacement response to axial cyclic loading of driven piles in sand

Réponse en déplacement au chargement cyclique axial de pieux battus dans le sable

Rimoy S., Jardine R., Standing J.
Imperial College London

ABSTRACT: Interactive axial cyclic loading stability charts have been developed to guide the assessment of axial cyclic capacity degradation of piles driven in sands. Less guidance is available regarding displacement accumulation and cyclic stiffness response at full scale. This paper focuses on axial cycling experiments of six full–scale steel open–ended pipe–piles at a marine sand site in Dunkerque, France. Multiple suites of cyclic loading were applied, interspersed with reference static tension capacity tests. The piles' stable, meta-stable and unstable capacity responses are identified with reference to a site-specific normalised cyclic interaction stability diagram. The stiffness response and rates of accumulated displacement associated with each style of cycling are reported. It is shown that under stable loading, the piles' cyclic stiffnesses remain constant or decline marginally. Similar trends are observed with meta-stable tests up to onset of an eventual cyclic failure, after which stiffness degrades rapidly. Unstable tests displayed shorter periods of modest change before marked losses of cyclic stiffness. The patterns of accumulated displacement growth show more complex relationships with the cyclic loading parameters that can be expressed in multi-surface 3-D plots.

RÉSUMÉ : Des diagrammes interactifs de stabilité cyclique ont été développés afin d'évaluer la dégradation cyclique des pieux battus dans les sables. Peu de données sont disponibles à échelle réelle en ce qui concerne les déplacements. Cet article s'intéresse aux essais cycliques axiaux de six pieux tubulaires en acier à base ouverte dans un site de sable marin à Dunkerque. Plusieurs séries de chargement cyclique ont été appliquées, entrecoupées d'essais statiques référentiels en traction. Les réponses stable, méta-stable et instable de capacité des pieux sont identifiées en relation avec un diagramme normalisé de stabilité cyclique. La réponse en termes de rigidité et de taux de déplacement accumulé associée à chaque type de chargement cyclique est ensuite présentée. On montre que sous un chargement stable, la rigidité cyclique reste constante ou diminue légèrement. On observe des tendances similaires dans les essais méta-stables jusqu'à l'apparition d'une éventuelle rupture cyclique, après laquelle la rigidité se dégrade rapidement. Les essais instables ont montré de courtes périodes de léger changement avant de fortes pertes de rigidité cyclique. Les schémas de croissance des déplacements cumulés montrent des relations avec les paramètres de charge cyclique plus complexes qui peuvent être exprimées dans des représentations 3-D.

KEYWORDS: axial cyclic loading/ pile stiffness/ accumulated displacements/ offshore engineering/ renewable energy
MOTS-CLÉS: chargement cyclique axial/rigidité du pieu/déplacements cumulés/ingénierie offshore/énergies renouvelables

1 INTRODUCTION

The axial cyclic response of driven pile foundations can be critical in the design of offshore oil and gas platforms, and multi-piled wind turbines, towers and pylons. Lateral and moment loads imposed by wind or wave action can be large compared to self-weights, leading to multiple modes of axial and lateral cyclic loading on the foundation piles. Lateral loading model tests have been reported that tracked the gradual rotation and stiffness of monopiles (Leblanc et al. 2010); however less guidance is available on full-scale displacement accumulation and stiffness responses under axial cycling.

Jardine et al. (2012) reviewed the potential effects of cyclic loading on offshore pile foundations and considered how these may be addressed in practical design for a range of geomaterials. They note that loads vary with platform weight, water depth, metocean environment and structural form. Of the 15 field research studies they identified, only one concerned silica sands, that at Dunkerque, France reported by Jardine & Standing (2000, 2012). Merritt et al. (2012) describe how the most severe tens or hundreds of cycles imposed in storms are the most critical to pile performance. The Jardine & Standing (2000) field study investigated behaviour up to 1000 cycles.

Karlsrud et al. (1986), Poulos (1988) and Jardine & Standing (2000) have used cyclic stability diagrams to guide the assessment of pile axial cyclic behaviour. These consider the interaction effects of cyclic and mean loads (normalised by static capacity before cycling) and the number of cycles applied. Such interaction diagrams may be zoned to identify a cyclically stable (S) region where there is no reduction of load capacity after N cycles, a meta-stable (MS) region where some reduction of load capacity occurs after N cycles and an unstable (US) region where cyclic failure develops within a small specified number of cycles. Jardine & Standing (2012) used a similar scheme in interpretation of their field tests at Dunkerque (Figure 1) where multiple cyclic loading tests performed that were interspersed with reference static tension capacity (Q_T) tests.

This paper focuses on further interpretation of the same axial cycling experiments. The axial static and cyclic stiffness responses are discussed and the accumulated cyclic displacement trends associated with each mode of cycling are examined, referring to the site specific normalised cyclic interaction stability diagram.

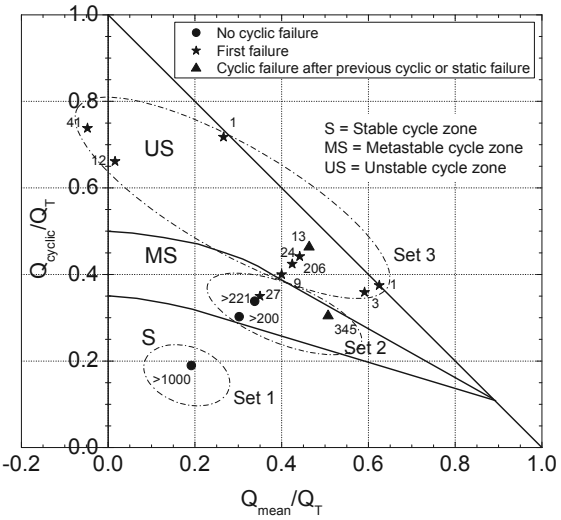

Figure 1. Axial cyclic interaction diagram for the full–scale pile tests in Dunkerque silica marine sands (Jardine & Standing 2012).

2 SCOPE OF STUDY

Seven full-scale 457mm diameter, 13.5mm wall thickness (increased to 20mm over top 2.5m), open-ended steel pipe-piles, six (R1 – R6) with embedded lengths around 19m and one (C1) driven to 10m were installed as part of the Grouted Offshore Piles for Alternating Loading (GOPAL) project (Parker et al. 1999) in a flat area close to Dunkerque Port Ouest Industrial Zone. The site has a relatively deep profile of dense sand, Figure 2. Chow (1997) reported static and cyclic pile tests incorporating pore pressure measurements that showed a fully drained response over the loading rates applied. The piles' cyclic capacity trends have been reported by Jardine and Standing (2000, 2012), while Jardine et al. (2006) reported the static tension capacity–time trends.

3 TEST PROGRAMME

Jardine et al. (2006) detail the testing arrangements, pile head load control and displacement measurements. The cyclic test programme is detailed on Table 1; load cycles were performed with periods between 1 to 2 minutes depending on the pile response. The axial cyclic load was applied in approximately sine wave forms as defined in Figure 3. The load-controlled tests involving only tensile pile head loads are termed 'one–way' while cycles ranging from tension to compression are referred to as 'two–way'; tension loads and upward displacement responses are taken as positive throughout. Reference static tension tests to failure were conducted after most of the cyclic tests to assess the effects on the applied axial cyclic loading on the operational static tension (shaft) capacity and isolate any effects of previous (static or cyclic) loading phases from the current axial cyclic behaviour.

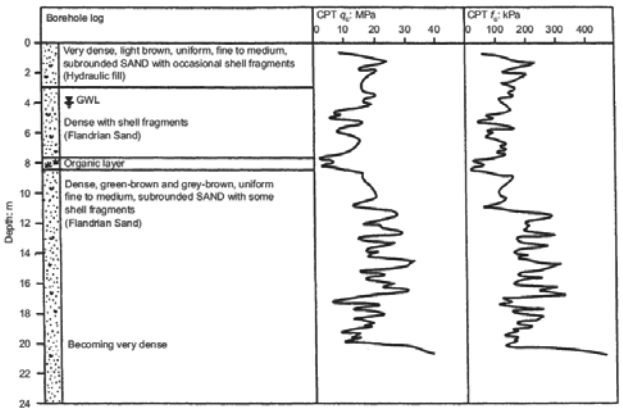

Figure 2. Typical site profile for Imperial College test site (Chow 1997)

4 RESULTS AND INTERPRETATION

4.1 *Cyclic failure criteria*

The axial cycling displacement response is classified as stable (S), meta–stable (MS) or unstable (US) according to the following criteria. *Stable* response signifies low and stabilising cyclic displacements that remain below 0.01 the pile diameter, D, and show slow rates of change ≤ 1mm/1000 cycles (N) up to N ≥ 1000 without causing loss in operational static shaft capacity. Tests with *meta–stable* responses accumulate > 0.01D displacements but < 0.1D with moderate rates (1mm/1000 cycles < rates ≤ 1mm/10 cycles) potentially leading to some degradation of the operational static shaft capacity but not causing failure within 100 cycles. *Unstable* responses lead to cyclic failure within 100 cycles, involving either accumulated permanent cyclic displacements > 0.1D or rates of accumulation of permanent cyclic displacements that exceed 1mm/10cycles with potentially very significant shaft degradation.

The fourteen cyclic tests gave a range of outcomes with one stable (set 1), four meta–stable (set 2) and nine unstable (set 3) responses indicated in Figure 1. The following sections analyse the cyclic stiffnesses and accumulated displacements seen in these three modes using the terms defined in Figure 4.

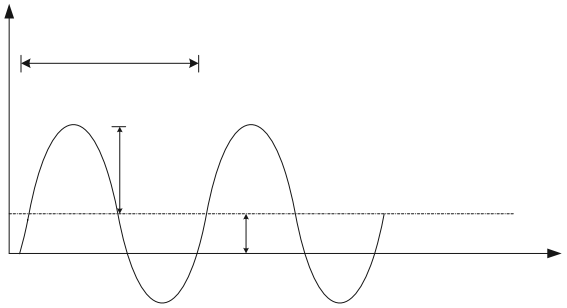

Figure 3. Load–controlled axial cycling illustrated (Tsuha et al. 2012)

4.2 *Pile axial cyclic stiffness*

The variations of the piles' secant stiffness, $k = \Delta Q/\Delta s$, under first-time static tension loading are shown on Figure 5 represented by the stiffnesses ratio, k/k_{Ref}, against the load ratio, Q/Q_{Ref}, where k_{Ref} is the pile stiffness at the first monotonic load step, Q_{Ref}, in the first-time tension tests. The 19m long piles (R2 to R6) follow common trends although one 'younger' and lower ultimate capacity 19m long pile R1 degraded more rapidly than the others as did the shorter (10m long) pile C1.

Table 1. Axial cyclic loading test programme: after Jardine & Standing (2000)

Test mode	Test code	Q_{cyclic} (kN)	Q_{mean} (kN)	Q_T (kN)	N_f
One–way	US 3.R2.CY2	1000	1000	2500	9
	MS 2.R3.CY2	700	700	2315	200+
	US 2.R3.CY3	950	950	2050	13
	MS 2.R4.CY2	1000	1000	2960	221+
	US 2.R4.CY4	750	1250	2000	3
	S 3.R4.CY6	400	405	2110	1000+
	MS 2.R5.CY2	750	1250	2465	345
	US 2.R5.CY3	700	700	2000	27
	US 2.R6.CY2	750	1250	2000	1
	US 2.R6.CY4	700	700	1585	24
	MS 3.R6.CY6	700	700	1650	206
Two–way	US 2.C1.CY3	620	-40	840	41
	US 2.C1.CY4	445	165	620	1
	US 2.C1.CY5	410	10	620	12

Test code explanation:
XX M.YY.ZZN:
XX = Pile response mode (S - Stable, MS – Meta-stable, US – Unstable)
M = Testing campaign phase (out of 3)
YY = Pile name (C1, R2 – R6)
ZZ = Test type (T – Static tension, C - Static compression, CY – Axial cyclic)
N = Test number on the pile in sequence from installation

Figure 6 examines the axial cyclic stiffness trends for the stable and meta–stable (sets 1 & 2 on Figure 1). The initial normalised stiffness values (i.e. k_I/k_{Ref} at N = 1) generally decreases as the proportion of applied Q_{max} to Q_T increases. In the stable loading test 3.R4.CY6, it can be seen that continued cycling leads to only a marginal stiffness decrease (12%) over 1000 cycles, with stiffness values stabilising and then marginally increasing after 200 cycles. Compared with this, the four meta–stable loading tests showed similarly mild stiffness degradation before manifesting sharply accelerating stiffness degradation as the piles approached cyclic failure under the conditions given in Table 1.

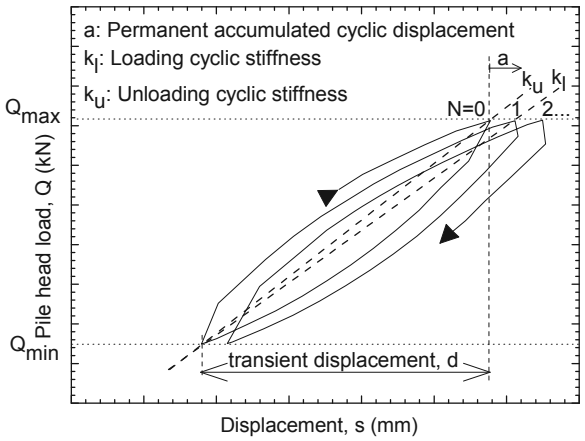

Figure 4. Illustration of the stiffness and displacement parameters used in the analyses

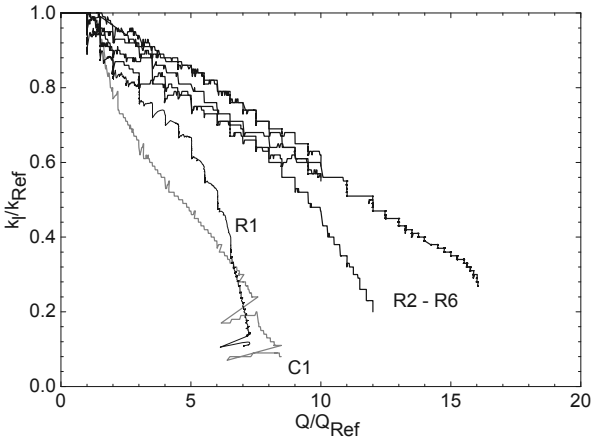

Figure 5. Pile stiffness from the first–time axial static monotonic tension loadings normalised by the reference stiffnesses against normalised load

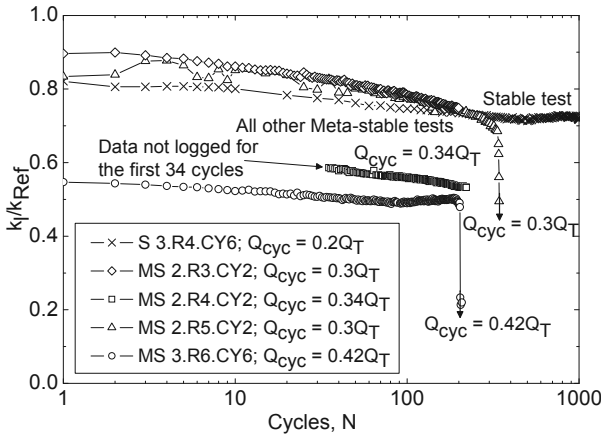

Figure 6. Axial cyclic loading stiffness k_l responses normalised by k_{Ref} against number of cycles for the stable and meta–stable tests.

The loading stiffness k_l degradation trends for the unstable tests (Set 3 of Figure 1) are shown on Figure 7. By definition, these tests failed with sudden stiffness loss after relatively few cycles. However, even these piles retained most of their initial stiffnesses until within ~10 cycles of final failure. Seemingly anomalous stiffness behaviour is observed towards failure in some one–way meta-stable and unstable loading tests when stiffnesses are defined from the unloading cycle phase k_u, Figure 8. This reversal in normalised stiffness results from an increased opening-up of the load-unload hysteresis loops as cyclic failure approaches with more plastic displacements accumulating on the loading loops leading to the progressively decreasing secant loading stiffnesses and apparently stiffer behaviour on unloading as cyclic loading approaches failure.

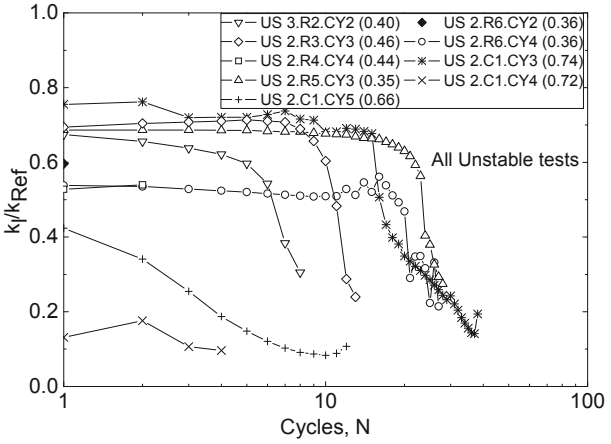

Figure 7. Axial cyclic loading stiffness k_l responses normalised by k_{Ref} against number of cycles for the unstable tests.

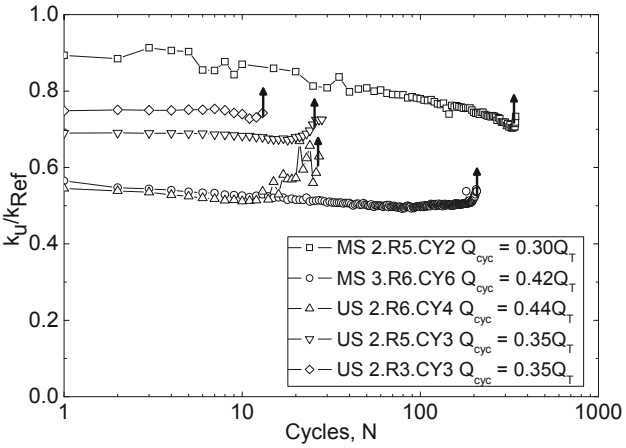

Figure 8. Axial cyclic unloading stiffness k_u responses normalised by k_{Ref} against number of cycles for selected metastable and unstable tests.

4.3 Accumulated cyclic displacements

The patterns of pile head displacement accumulation for the stable and meta–stable cyclic tests are shown on Figure 9. Also shown are the reference lines related to the predefined thresholds for stable, metastable and unstable accumulated displacements rates. An almost static accumulated displacement trend was observed in the single fully stable loading test 3.R4.CY6. The meta–stable tests 2.R3.CY2 and 2.R4.CY2 developed higher, but steady displacement rates > 1mm/100cycles while the other two meta–stable tests 2.R5.CY2 and 3.R6.CY6 displaced by > 1mm/10cycles. A range of responses is evident for the unstable loading tests summarised in Figure 10 which develop displacement rates > 1mm/10cycles.

While the cyclic stiffness patterns varied principally as a function of the applied cyclic amplitudes Q_{cyclic}, the accumulated cyclic displacement patterns depended on both the normalised mean (Q_{mean}/Q_T) and cyclic (Q_{cyclic}/Q_T) loads. Rimoy et al. (2013) demonstrate the interactive effects of the loading components Q_{cyclic} and Q_{mean} by considering the accumulated displacements developed after 3, 10, 30, 100, 200, and 300 cycles to produce tentative 3D surfaces equivalent to displacements of 2%, 0.2% or 0.02% pile diameter, Figure 11. The accumulated displacement trends flatten progressively as N increases. The zero cyclic effect boundary was set at Q_{cyclic}/Q_T =

0.1 following centrifuge studies by Julio (2009). No displacements are expected to accrue due to cycling below this level; further full-scale specific investigation of this lower threshold is required.

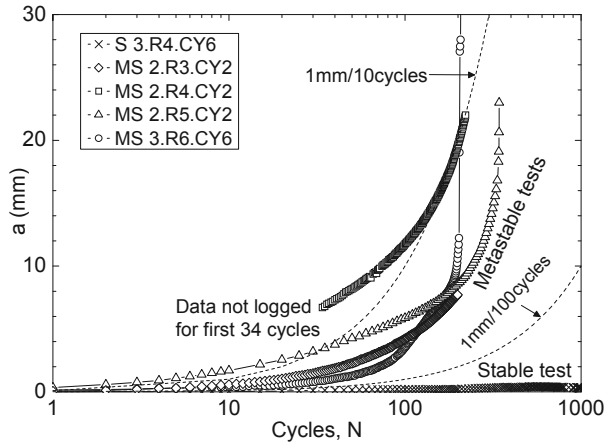

Figure 9. Accumulated cyclic displacements for the stable and meta–stable loading tests

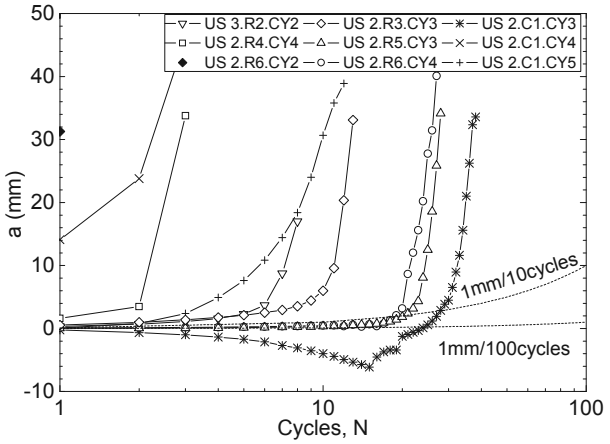

Figure 10. Permanent accumulated cyclic displacements response for the unstable tests

5 SUMMARY AND CONCLUSIONS

The analysis presented of the axial cyclic loading load–displacement, stiffness and accumulated displacements responses seen in tests on steel open-ended pipe piles driven in silica sand indicate the following.

(1) Axial load–displacement behaviour is highly non-linear, even at relatively low levels of loading.

(2) The piles' cyclic stiffnesses generally remained within 20% of those observed under initial static loading until cyclic failure was approached.

(3) The patterns of accumulated displacements depended on both the mean and cyclic normalised loading levels.

(4) While displacements accumulate rapidly over just a few cycles in the unstable zone, extended cycling in the stable zone led to minimal (and stabilising) accumulated displacements and axial capacity gains (Jardine et al (2006) meta–stable tests showed intermediate behaviour.

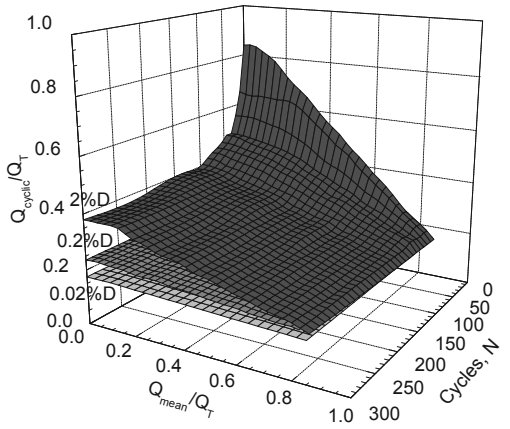

Figure 11. 3D plot for accumulated cyclic displacements equivalent to 0.02%D, 0.2%D and 2%D.

6 ACKNOWLEDGEMENTS

The above research was funded by the EU (through the GOPAL project) and Health and Safety Executive (HSE) of UK. We gratefully acknowledge the Port Autonome de Dunkerque for providing the test site. The field testing was conducted in conjunction with Precision Monitoring Control Ltd. of Teesside UK. The first author has been supported by the Commonwealth Scholarship Commission during the writing of this paper.

7 REFERENCES

Chow F.C. 1997. *Investigations into displacement pile behaviour for offshore foundations,* PhD thesis, University of London (Imperial College).

Jardine R.J. & Standing J.R. 2000. *Pile load testing performed for HSE cyclic loading study at Dunkirk, France.* Two volumes. Offshore Technology Report OTO2000 007; Health and Safety Executive, London. 60p and 200p.

Jardine, R.J., Standing, J.R., & Chow, F.C. 2006. Some observations of the effects of time on the capacity of piles driven in sand. *Géotechnique* 56(4): 227-244.

Jardine R.J. & Standing J.R. 2012. Field axial cyclic loading experiments on piles driven sand. *Soils and foundations* 52(4): 723 - 736.

Jardine R.J., Puech A. & Andersen K. H. 2012. Cyclic loading of offshore piles: Potential effects and practical design. *Proceedings of the SUT 7th International Conference on Offshore Site Investigation and Geotechnics*, London, UK, pp. 59 - 97.

Julio R.M.H. 2009. *Comportement des pieux et des groupes de pieux sous chargement latéral cyclique.* These de doctorat, Ecole Nationale des Ponts et Chaussees, Paris, France.

Karlsrud K., Nadim F. & Haugen T. 1986. Piles in clay under cyclic axial loading field test and computational modelling. *Proceedings of the 3rd International Conference on Numerical Methods in Offshore Piling*, Nantes, France, pp. 165 – 190.

Leblanc C., Houlsby G.T., & Bryne B.W. 2010. Response of stiff piles in sand to long-term cyclic lateral loading. *Géotechnique* 60(2): 79-90.

Merritt A.S., Schroeder F.C., Jardine R.J., Stuyts B., Cathie D. & Cleverly D. 2012. Development of pile design methodology for an offshore wind farm in the North Sea. *Proceedings of the SUT 7th International Conference on Offshore Site Investigation and Geotechnics,* London, UK, pp. 439 - 447.

Parker E. J., Jardine R.J., Standing J.R. & Xavier J. 1999. Jet grouting to improve offshore pile capacity. *Offshore Technology Conference, Houston, OTC 10828* 1: 415 – 420.

Poulos H.G. 1988. Cyclic stability diagram for axially loaded piles. *Journal of Geotechnical and Geoenvironmental Engineering,* 114(8): 877-895.

Rimoy S., Jardine R., and Standing J. 2013. Displacement response to axial cycling of piles driven in sand. *Geotechnical Engineering*. 165 (GE1): 1 – 16.